Cubic Topological Kondo Insulators

Victor Alexandrov,[1] Maxim Dzero,[2] and Piers Coleman[1,3]

[1]*Department of Physics and Astronomy, Center for Materials Theory, Rutgers University, Piscataway, New Jersey 08854-8019, USA*
[2]*Department of Physics, Kent State University, Kent, Ohio 44242, USA*
[3]*Department of Physics, Royal Holloway, University of London, Egham, Surrey TW20 0EX, United Kingdom*

(Received 30 April 2013; revised manuscript received 12 September 2013; published 27 November 2013)

Current theories of Kondo insulators employ the interaction of conduction electrons with localized Kramers doublets originating from a tetragonal crystalline environment, yet all Kondo insulators are cubic. Here we develop a theory of cubic topological Kondo insulators involving the interaction of Γ_8 spin quartets with a conduction sea. The spin quartets greatly increase the potential for strong topological insulators, entirely eliminating the weak topological phases from the diagram. We show that the relevant topological behavior in cubic Kondo insulators can only reside at the lower symmetry X or M points in the Brillouin zone, leading to three Dirac cones with heavy quasiparticles.

DOI: 10.1103/PhysRevLett.111.226403 PACS numbers: 71.27.+a, 71.28.+d, 72.15.Qm, 75.20.Hr

Our classical understanding of order in matter is built around Landau's concept of an order parameter. The past few years have seen a profound growth of interest in topological phases of matter, epitomized by the quantum Hall effect and topological band insulators, in which the underlying order derives from the nontrivial connectedness of the quantum wave function, often driven by the presence of strong spin-orbit coupling [1–9].

One of the interesting new entries to the world of topological insulators is the class of heavy fermion or "Kondo insulators" [10–16]. The strong-spin orbit coupling and highly renormalized narrow bands in these intermetallic materials inspired the prediction [12] that a subset of the family of Kondo insulators will be Z_2 topological insulators. In particular, the oldest known Kondo insulator SmB_6 [17] with marked mixed valence character, was identified as a particularly promising candidate for a strong topological insulator, a conclusion that has since also been supported by renormalized band theory[13,16]. Recent experiments [18–20] on SmB_6 have confirmed the presence of robust conducting surfaces, large bulk resistivity, and a chemical potential that clearly lies in the gap providing strong support for the initial prediction.

However, despite these developments, there are still many aspects of the physics in these materials that are poorly understood. One of the simplifying assumptions of the original theory [12] was to treat the f states as Kramer's doublets in a tetragonal environment. In fact, the tetragonal theory predicts that strong topological insulating behavior requires large deviations from integral valence, while in practice Kondo insulators are much closer to integral valence [11]. Moreover, all known Kondo insulators have cubic symmetry, and this higher symmetry appears to play a vital role, for all apparent "Kondo insulators" of lower symmetry, such as CeNiSn [21] or $CeRu_4Sn_6$ [22], have proven, upon improving sample quality, to be semimetals. One of the important effects of high symmetry is the stablization of magnetic f quartets. Moreover, Raman [23] experiments and various band-theory studies [24,25] indicate that it is the Kondo screening of the magnetic quartets that gives rise to the emergence of the insulating state.

Motivated by this observation, here we formulate a theory of cubic topological Kondo insulators, based on a lattice of magnetic quartets. We show that the presence of a spin quartet greatly increases the possibility of strong topological insulators while eliminating the weak topological insulators from the phase diagram, Fig. 1. We predict that the relevant topological behavior in simple cubic Kondo insulators can only reside at the lower point group symmetry X and M points in the Brillouin zone, leading to three heavy Dirac cones at the surface. One of the additional consequences of the underlying Kondo physics is that the coherence length of the surface states is expected to be very small, of the order of a lattice spacing.

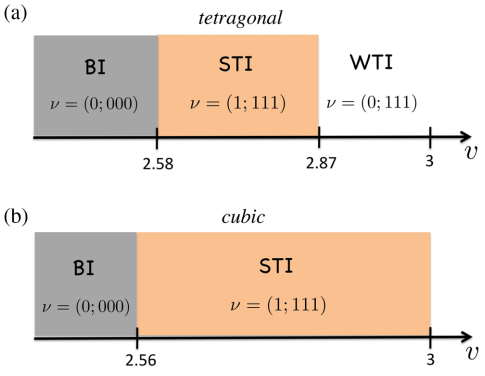

FIG. 1 (color online). Contrasting the phase diagram of (a) tetragonal [27] and (b) cubic topological Kondo insulators. Cubic symmetry extends the strong topological insulator phase into the Kondo limit. For SmB_6 $v = 3 - n_f$ gives the valence of the Sm ion, while n_f measures the number of f holes in the filled $4f^6$ state, so that $n_f = 1$ corresponds to the $4f^5$ configuration.

While we outline our model of cubic Kondo insulators with a particular focus on SmB_6, the methodology generalizes to other cubic Kondo insulators. SmB_6 has a simple cubic structure, with the B_6 clusters located at the center of the unit cell acting as spacers that mediate electron hopping between Sm sites. Band theory [25] and XPS studies [26] show that the $4f$ orbitals hybridize with d bands, which form electron pockets around the X points. In a cubic environment, the $J = 5/2$ orbitals split into a Γ_7 doublet and a Γ_8 quartet, while the fivefold degenerate d orbitals are split into double degenerate e_g and triply degenerate t_{2g} orbitals. Band theory and Raman spectroscopy studies [23] indicate that the physics of the $4f$ orbitals is governed by valence fluctuations involving electrons of the Γ_8 quartet and the conduction e_g states, $e^- + 4f^5(\Gamma_8^{(\alpha)}) \rightleftharpoons 4f^6$. The $\Gamma_8^{(\alpha)}$ ($\alpha = 1, 2$) quartet consists of the following combination of orbitals: $|\Gamma_8^{(1)}\rangle = \sqrt{\frac{5}{6}}|\pm\frac{5}{2}\rangle + \sqrt{\frac{1}{6}}|\mp\frac{3}{2}\rangle$, $|\Gamma_8^{(2)}\rangle = |\pm\frac{1}{2}\rangle$. This then leads to a simple physical picture in which the Γ_8 quartet of f states hybridizes with an e_g *quartet* (Kramers plus orbital degeneracy) of d states to form a Kondo insulator.

To gain insight into how the cubic topological Kondo insulator emerges, it is instructive to consider a simplified one-dimensional model consisting of a quartet of conduction d bands hybridized with a quartet of f bands [Fig. 2(a)]. In one dimension there are two high symmetry points, Γ ($k = 0$) and X ($k = \pi$), where the hybridization vanishes [12,14,27]). Away from the zone center Γ, the $f-$ and $d-$ quartets split into Kramers doublets. The Z_2 topological invariant ν_{1D} is then determined by the product of the parities $\nu_{1D} = \delta_\Gamma \delta_X$ of the occupied states at the Γ and X points. However, the f quartet at the Γ point is equivalent to two Kramers doublets, which means that $\delta_\Gamma = (\pm 1)^2$ is always positive, so that $\nu_{1D} = \delta_X$ and a one-dimensional topological insulator only develops when the f and d bands invert at the X point.

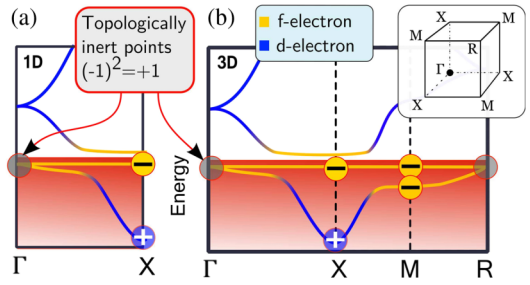

FIG. 2 (color online). Schematic band structure illustrating (a) one-dimensional Kondo insulator with local cubic symmetry and (b) three-dimensional cubic Kondo insulator. Hybridization between a quartet of d bands with a quartet of f bands leads to a Kondo insulator. The fourfold degeneracy of the f and d bands at the high symmetry Γ and R points of the Brillouin zone guaranties that the three-dimensional topological invariant is determined by the band inversions at the X and M points only.

Generalizing this argument to three dimensions, we see that there are now four high symmetry points Γ, X, M and R. The f bands are fourfold degenerate at both Γ and R points, which guarantees that $\delta_\Gamma = \delta_R = +1$ [Fig. 2(b)]. Therefore, we see that the three-dimensional topological invariant is determined by band inversions at X or M points only, $\nu_{3D} = (\delta_X \delta_M)^3 = \delta_X \delta_M$. If there is a band inversion at the X point, we get $\nu_{3D} = \delta_X \delta_M = -1$. In this way the cubic character of the Kondo insulator and, specifically, the fourfold degeneracy of the f-orbital multiplet protects the formation of a strong topological insulator.

We now formulate our model for cubic topological Kondo insulators. At each site, the quartet of f and d holes is described by an orbital and spin index, denoted by the combination $\lambda \equiv (a, \sigma)$ ($a = 1, 2$, $\sigma = \pm 1$). The fields are then given by the eight-component spinor

$$\Psi_j = \begin{pmatrix} d_\lambda(j) \\ X_{0\lambda}(j) \end{pmatrix}, \tag{1}$$

where $d_\lambda(j)$ destroys a d hole at site j, while $X_{0\lambda}(j) = |4f^6\rangle\langle 4f^5, \lambda|$ is the Hubbard operator that destroys an f hole at site j. The tight-binding Hamiltonian describing the hybridized f-d system is then

$$H = \sum_{i,j} \Psi_\lambda^\dagger(i) h_{\lambda\lambda'}(\mathbf{R}_i - \mathbf{R}_j) \Psi_{\lambda'}(j), \tag{2}$$

in which the nearest hopping matrix has the structure

$$h(\mathbf{R}) = \begin{pmatrix} h^d(\mathbf{R}) & V(\mathbf{R}) \\ V^\dagger(\mathbf{R}) & h^f(\mathbf{R}) \end{pmatrix}, \tag{3}$$

where the diagonal elements describe hopping within the d and f quartets, while the off-diagonal parts describe the hybridization between them and $\mathbf{R} \in (\pm\hat{\mathbf{x}}, \pm\hat{\mathbf{y}}, \pm\hat{\mathbf{z}})$ is the vector linking nearest neighbors. The various matrix elements simplify for hopping along the z axis, where they become orbitally and spin diagonal,

$$h^l(\mathbf{z}) = t^l \begin{pmatrix} 1 & \\ & \eta_l \end{pmatrix}, \qquad V(\mathbf{z}) = i\frac{V}{2} \begin{pmatrix} 0 & \\ & \sigma_z \end{pmatrix}, \tag{4}$$

where $l = d$, f and η_l is the ratio of orbital hopping elements. In the above, the overlap between the $\Gamma_8^{(1)}$ orbitals, which extend perpendicular to the z axis, is neglected, since the hybridization is dominated by the overlap of the $\Gamma_8^{(2)}$ orbitals, which extend out along the z axis. The hopping matrix elements in the $\mathbf{x}$ and $\mathbf{y}$ directions are then obtained by rotations in orbital or spin space, so that $h(\mathbf{x}) = U_y h(\mathbf{z}) U_y^\dagger$ and $h(\mathbf{y}) = U_{-x} h(\mathbf{z}) U_{-x}^\dagger$, where U_y and U_{-x} denote 90° rotations about the y and negative x axes, respectively.

The Fourier transformed hopping matrices $h(\mathbf{k}) = \sum_{\mathbf{R}} h(\mathbf{R}) e^{-i\mathbf{k}\cdot\mathbf{R}}$ can then be written in the compact form

$$h^l(\mathbf{k}) = \frac{t^l}{2}\begin{pmatrix} \phi_1(\mathbf{k}) + \eta_l\phi_2(\mathbf{k}) & (1-\eta_l)\phi_3(\mathbf{k}) \\ (1-\eta_l)\phi_3(\mathbf{k}) & \phi_2(\mathbf{k}) + \eta_l\phi_1(\mathbf{k}) \end{pmatrix} + \epsilon^l, \tag{5}$$

where $l = d, f$. Here ϵ^l are the bare energies of the isolated d and f quartets, while $\phi_1(\mathbf{k}) = c_x + c_y + 4c_z$, $\phi_2(\mathbf{k}) = 3(c_x + c_y)$, and $\phi_3(\mathbf{k}) = \sqrt{3}(c_x - c_y)$ ($c_\alpha \cos k_\alpha$, $\alpha = x, y, z$). The hybridization is given by

$$V(\mathbf{k}) = \frac{V}{4}\begin{pmatrix} -3(\bar{\sigma}_x + \bar{\sigma}_y) & \sqrt{3}(\bar{\sigma}_x - \bar{\sigma}_y) \\ \sqrt{3}(\bar{\sigma}_x - \bar{\sigma}_y) & -(\bar{\sigma}_y + \bar{\sigma}_x) + 4\bar{\sigma}_z) \end{pmatrix}, \tag{6}$$

where we denote $\bar{\sigma}_\alpha = \sigma_\alpha \sin k_\alpha$. Note how the hybridization between the even parity d states and odd-parity f states is an odd parity function of momentum $V(\mathbf{k}) = -V(-\mathbf{k})$.

To analyze the properties of the Kondo insulator, we use a slave boson formulation of the Hubbard operators, writing $X_{\lambda 0}(j) = f^\dagger_\lambda(j) b_j$, where $f^\dagger_\lambda|0\rangle \equiv |4f^5, \lambda\rangle$ creates an f hole in the Γ^8 quartet, while $b^\dagger|0\rangle \equiv |4f^6\rangle$ denotes the singlet filled $4f$ shell, subject to the constraint $Q_j = b^\dagger_j b_j + \sum_\lambda f^\dagger_{j\lambda} f_{j\lambda} = 1$ at each site.

We now analyze the properties of the cubic Kondo insulator, using a mean-field treatment of the slave boson field b_i, replacing the slave-boson operator $\hat{b}_i$ at each site by its expectation value $\langle \hat{b}_i \rangle = b$ so that the f-hopping and hybridization amplitude are renormalized, $t_f \to b^2 t_f$ and $V_{df} \to b V_{df}$. The mean-field theory is carried out, enforcing the constraint $b^2 + \langle n_f \rangle = 1$ on the average. In addition, the chemical potentials ϵ_d and ε_f for both d electrons and f holes are adjusted self-consistently to produce a band insulator, $n_d + n_f = 4$. This condition guarantees that four out of eight doubly degenerate bands will be fully occupied. The details of our mean-field calculation are given in the Supplemental Material [28] section. Here we provide the final results of our calculations.

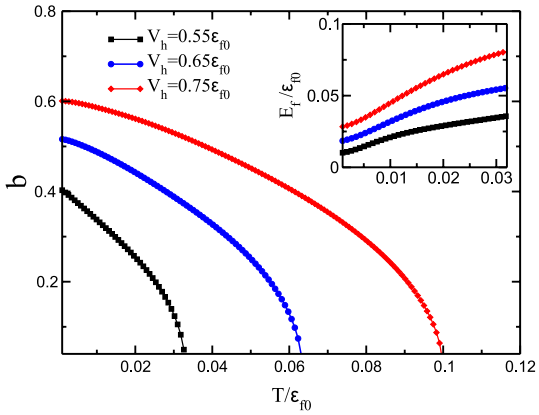

FIG. 3 (color online). Temperature dependence of the hybridization gap parameter b and the renormalized f-level position (inset) for various values of the bare hybridization (see Supplemental Material [28] for more details).

In Fig. 3 we show that the magnitude b reduces with temperature, corresponding to a gradual rise in the Sm valence, due to the weaker renormalization of the f-electron level. The degree of mixed valence of Sm^+ is given then by $v = 3 - \langle n_f \rangle$. In our simplified mean-field calculation, the smooth temperature crossover from Kondo insulating behavior to local moment metal at high temperatures is crudely approximated by an abrupt second-order phase transition.

Figure 4 shows the computed band structure for the cubic Kondo insulator obtained from mean-field theory, showing the band inversion between the d and f bands at the X points that generates the strong topological insulator. Moreover, as the value of the bare hybridization increases, there is a maximum value beyond which the bands no longer invert and the Kondo insulator becomes a conventional band insulator.

One of the interesting questions raised by this work concerns the many-body character of the Dirac electrons on the surface. Like the low-lying excitations in the valence and conduction band, the surface states of a TKI involve heavy quasiparticles of predominantly f character. The characteristic Fermi velocity of these excitations $v^*_F = Z v_F$ is renormalized with respect to the conduction electron band group velocities, where $Z = m/m^*$ is the mass renormalization of the f electrons. In a band topological insulator, the penetration depth of the surface state is $\xi \sim v_F/\Delta$, where Δ is the band gap, a scale that is significantly larger than a unit-cell size. Paradoxically, even though the Fermi velocity of the Dirac cones in a TKI is very low, we expect the characteristic penetration depth ξ of the heavy wave functions into the bulk to be of order the lattice spacing a. To see this, we note that $\xi \sim (v^*_F/\Delta_g)$, where the indirect gap of the Kondo insulator Δ_g is of order the Kondo temperature $\Delta_g \sim T_K$. But since

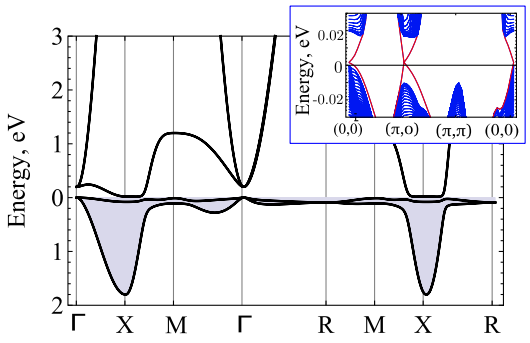

FIG. 4 (color online). Band structure consistent with PES and LDA studies of SmB_6 computed with the following parameters: $n_f = 0.48$ (or $b = 0.73$), $V = 0.4$ eV, $t_d = 2$ eV, $\mu_d = 0.2$ eV, $\eta = \eta' = -.3$, $\epsilon_f = -0.01$ eV ($\epsilon_{f0} = -0.17$ eV), $t_f = -.05$ eV, $T = 10^{-4}$ eV, and the gap is $\Delta = 12$ meV. Shaded region denotes filled bands. Inset shows the ground-state energy computed for a slab of 80 layers to illustrate the three gapless surface Dirac excitations at the symmetry points $\hat{\Gamma}$, $\hat{X}'$, and X''.

$T_K \sim ZW$, where W is the width of the conduction electron band, this implies that the penetration depth of the surface excitations $\xi \sim v_F/W \sim a$ is given by the size a of the unit cell. Physically, we can interpret the surface Dirac cones as a result of broken Kondo singlets, whose spatial extent is of order a lattice spacing. This feature is likely to make the surface states rather robust against the purity of the bulk.

Various interesting questions are raised by our study. Conventional Kondo insulators are most naturally understood in the strong-coupling limit of the Kondo lattice, where local singlets form between a commensurate number of conduction electrons and localized moments. What then is the appropriate strong coupling description of topological Kondo insulators, and can we understand the surface states in terms of broken Kondo singlets? A second question concerns the temperature dependence of the hybridization gap. Experimentally, the hybridization gap observed in Raman and transport studies [23,29] is seen to develop in a fashion strongly reminiscent of the mean-field theory. Could this close resemblance to the mean-field theory indicate that fluctuations about mean-field theory are weaker in a fully gapped Kondo lattice than in its metallic counterpart?

To summarize, we have studied the cubic topological Kondo insulator, incorporating the effect of a fourfold degenerate f multiplet. There are two main effects of the quartet states: first, that the quarter filling of the quartet allows the fractional filling of the band favorable to strong topological insulating behavior to occur in the almost integral valent environment of the Kondo insulator and, second, that doubling the degeneracy of the band states at the high-symmetry Γ and R points in the Brillouin zone, so that their net parity is always positive, effectively removes these points from the calculation of the Z_2 topological invariant so that the only important crossing must take place at the X or M points. For the cubic topological Kondo insulators, this immediately leads to a prediction that three heavy Dirac cones will form on the surfaces [13,16].

We would like to thank A. Ramires, V. Galitski, K. Sun, S. Artyukhin, and J. P. Paglione for stimulating discussions related to this work. This work was supported by the Ohio Board of Regents Research Incentive Program Grant No. OBR-RIP-220573 (M. D.), DOE Grant No. DE-FG02-99ER45790 (V. A. and P. C.), and the U.S. National Science Foundation I2CAM International Materials Institute Award, Grant No. DMR-0844115.

Note added.—After the submission of this Letter, several groups [30–33] have reported angular-resolved photoemission spectroscopy (ARPES) results that support the presence of surface states predicted by this and earlier papers [13,16]. In addition, torque magnetometry measurements [34] have observed de Haas–van Alphen oscillations associated with the surface states of SmB_6 that are consistent with a two-dimensional Dirac spectrum. The masses of the excitations seen in both sets of experiments are, however, significantly smaller than expected in the current theory. Lastly, experimental observations of weak antilocalization signatures in conductivity [35] as well as induced localization of the metallic surface states with an addition of magnetic impurities [36] provide strong circumstantial evidence that the surface quasiparticles are spin polarized, as expected in a topological insulator.

[1] L. Fu, C. L. Kane and E. J. Mele, Phys. Rev. Lett. **98**, 106803 (2007).
[2] J. E. Moore and L. Balents, Phys. Rev. B **75**, 121306(R) (2007).
[3] D. Hsieh, D. Qian, L. Wray, Y. Xia, Y. S. Hor, R. J. Cava, and M. Z. Hasan, Nature (London) **452**, 970 (2008).
[4] Y. Xia, D. Qian, D. Hsieh, L. Wray, A. Pal, H. Lin, A. Bansil, D. Grauer, Y. S. Hor, R. J. Cava, and M. Z. Hasan, Nat. Phys. **5**, 398 (2009).
[5] P. Roushan, J. Seo, C. V. Parker, Y. S. Hor, D. Hsieh, D. Qian, A. Richardella, M. Z. Hasan, R. J. Cava, and A. Yazdani, Nature (London) **460**, 1106 (2009).
[6] T. Zhang, P. Cheng, X. Chen, J. F. Jia, X. C. Ma, K. He, L. L. Wang, H. J. Zhang, X. Dai, Z. Fang, X. C. Xie, and Q. K. Xue, Phys. Rev. Lett. **103**, 266803 (2009).
[7] J. Seo, P. Roushan, H. Beidenkopf, Y. S. Hor, R. J. Cava, and A. Yazdani, Nature (London) **466**, 343 (2010).
[8] M. Z. Hasan and C. L. Kane, Rev. Mod. Phys. **82**, 3045 (2010).
[9] X.-L. Qi and S.-C. Zhang, Rev. Mod. Phys. **83**, 1057 (2011).
[10] G. Aeppli and Z. Fisk, Comments Condens. Matter Phys. **16**, 155 (1992).
[11] P. Riseborough, Adv. Phys. **49**, 257 (2000).
[12] M. Dzero, K. Sun, V. Galitski, and P. Coleman, Phys. Rev. Lett. **104**, 106408 (2010).
[13] T. Takimoto, J. Phys. Soc. Jpn. **80**, 123710 (2011).
[14] M. Dzero, K. Sun, P. Coleman, and V. Galitski, Phys. Rev. B **85**, 045130 (2012).
[15] M. T. Tran, T. Takimoto, and K. S. Kim, Phys. Rev. B **85**, 125128 (2012).
[16] F. Lu, J. Zhao, H. Weng, Z. Fang, and X. Dai, Phys. Rev. Lett. **110**, 096401 (2013).
[17] A. Menth, E. Buehler, and T. H. Geballe, Phys. Rev. Lett. **22**, 295 (1969).
[18] S. Wolgast, C. Kurdak, K. Sun, J. W. Allen, D. J. Kim, and Z. Fisk, arXiv:1211.5104.
[19] X. Zhang, N. P. Butch, P. Syers, S. Ziemak, R. L. Greene, and J. P. Paglione, Phys. Rev. X **3**, 011011 (2013).
[20] J. Botimer, D. J. Kim, S. Thomas, T. Grant, Z. Fisk, and J. Xin, Sci. Rep. **3**, 3150 (2013).
[21] K. Izawa, T. Suzuki, T. Fujita, T. Takabatake, G. Nakamoto, H. Fujii, and K. Maezawa, Phys. Rev. B **59**, 2599 (1999).
[22] S. Paschen, H. Winkler, T. Nezu, M. Kriegisch, G. Hilscher, J. Custers, and A. Prokofiev, J. Phys. Conf. Ser. **200**, 012156 (2010).
[23] P. Nyhus, S. L. Cooper, Z. Fisk, and J. Sarrao, Phys. Rev. B **55**, 12 488 (1997).

[24] A. Yanase and H. Harima, Prog. Theor. Phys. Suppl. **108**, 19 (1992).
[25] V. N. Antonov, B. N. Harmon, and A. N. Yaresko, Phys. Rev. B **66**, 165209 (2002).
[26] H. Miyazaki, T. Hajiri, T. Ito, S. Kunii, and S. I. Kimura, Phys. Rev. B **86**, 075105 (2012).
[27] M. Dzero, Eur. Phys. J. B **85**, 297 (2012).
[28] See Supplemental Material at http://link.aps.org/supplemental/10.1103/PhysRevLett.111.226403 for details of the tight-binding Hamiltonian and the mean-field theory.
[29] J. Derr, G. Knebel, D. Braithwaite, B. Salce, J. Flouquet, K. Flachbart, S. Gabáni, and N. Shitsevalova, Phys. Rev. B **77**, 193107 (2008).
[30] M. Neupane *et al.*, arXiv:1306.4634.
[31] J. Jiang *et al.*, arXiv:1306.5664.
[32] N. Xu *et al.*, arXiv:1306.3678.
[33] E. Frantzeskakis *et al.*, arXiv:1308.0151.
[34] G. Li *et al.*, arXiv:1306.5221.
[35] S. Thomas *et al.*, arXiv:1307.4133.
[36] D. J. Kim, J. Xia, and Z. Fisk, arXiv:1307.0448.